

Biogenic ZnO nanoparticles synthesized using *L. aculeata* leaf extract and their antifungal activity against plant fungal pathogens

S NARENDHRAN* and RAJESHWARI SIVARAJ

Department of Biotechnology, School of Life Sciences, Karpagam Academy of Higher Education, Eachanari Post, Coimbatore 641 021, India

MS received 3 September 2015; accepted 14 September 2015

Abstract. In this study, Zinc oxide (ZnO) nanoparticles were synthesized using aqueous extract of *Lantana aculeata* Linn. leaf and assessed their effects on antifungal activity against the plant fungal pathogens. Synthesized nanoparticles were confirmed by ultraviolet–visible spectroscopy, Fourier transform infrared spectrometer, energy-dispersive X-ray spectrometer, X-ray diffractometer, Field-emission scanning electron microscopy, high-resolution transmission electron microscopy. The antifungal activity of ZnO nanoparticles were determined using the well diffusion method. All the characterization analyses revealed that nanoparticles were highly stable and crystalline in nature. *L. aculeata*-mediated ZnO nanoparticles were spherical in shape with an average particle size of 12 ± 3 nm. Antifungal studies concluded that the maximum zone of inhibition was observed in *Aspergillus flavus* (21 ± 1.0 mm) and *Fusarium oxysporum* (19 ± 1.0 mm) at $100 \mu\text{g ml}^{-1}$ concentration. These results clearly indicated the benefits of using ZnO nanoparticles synthesized using biological methods and shown to have antifungal activities and also that it can be effectively used as antifungal agent in environmental aspect of agricultural development.

Keywords. Antifungal activity; FESEM; FTIR; HRTEM; *L. aculeata*; ZnO nanoparticles.

1. Introduction

Nanoparticles have gained increasing importance because of their novel properties, including a large specific surface area and high reaction activity [1,2]. Nanoparticles are atomic or molecular aggregates with at least one dimension from 1 to 100 nm that can drastically modify their physico-chemical properties compared with the bulk material [3–5]. Among the metal oxides, nano-zinc oxide (ZnO) exhibits wide band gap (~ 3.4 eV) and large exciton binding energy (60 meV) and thus it is considered as most promising candidate for nano-optoelectronics, sensors, transistors, nanopiezoelectronics and UV-detection [6]. ZnO is a II–VI semiconductor material due to its application on solar cells, gas sensors, ceramics and catalysts [7]. ZnO nanoparticles are widely used as an additive into numerous materials and products including paints, cosmetics, plastic and rubber manufacturing, electronics, pharmaceuticals as well as wide applications in agricultural and aquaculture [8].

The synthesis of nanoparticles by conventional physical and chemical methods has some adverse effects like critical conditions of temperature and pressure, expensive and toxic chemicals, long reflux time of reaction, toxic byproducts [9,10]. When compared to physical and chemical method, green synthesis of nanoparticles makes use of environmental friendly, non-toxic and safe reagents [11]. In recent times ZnO nanoparticles have been synthesized using the plant

extracts of *Eichhornia crassipes* and assessing its antifungal activity [12]. The effect of temperature on nanoparticle formation also has been investigated and it has been reported that polydisperse particles with a size range of 5–300 nm was obtained at lower temperature while a higher temperature supported the formation of much smaller and spherical particles [13]. Therefore compared to bacteria and fungi, plants are better candidates for the synthesis of nanoparticles [14].

Lantana aculeata (Family: Verbenaceae) is the major exotic weed, spreading rapidly on wastelands, stock poisoning, pose a threat to an environmentally significant area and invasion of desirable pasture. *L. aculeata* is a heavily branched, scrambling, thicket-forming shrub, usually ranging from 2 to 4 m in height [15,16]. Therefore, nanotechnology is alternate approach for controlling weed plant and management. In the present study, ZnO nanoparticles were synthesized from *L. aculeata* leaf extract and the antifungal activity was evaluated using the well diffusion method.

2. Materials and methods

2.1 Materials

Fresh, healthy and young *L. aculeata* leaves were collected from Vadavalli region (11.0100°N , 76.9000°E), Coimbatore, Tamil Nadu, India. The sample was authenticated by Botanical Survey of India, Coimbatore (BSI/SRC/5/23/2014-15/Tech/1418). All plant fungal pathogens such as *Aspergillus niger* (MTCC: 10180), *Fusarium oxysporum*

*Author for correspondence (narendhransumathi@gmail.com)

(MTCC: 3326, 3327, 3930) and *Penicillium funiculosum* (MTCC: 4888) were obtained from Institute of Microbial Technology, Chandigarh, India. All the chemicals were purchased from Sigma-Aldrich Chemicals, India.

2.2 Preparation of plant extract

Five grams of fresh leaves were weighed carefully and finely cut. Surfaces of the leaves were washed with running tap water, followed by distilled water. Leaves were ground well in a mortar and pestle using de-ionized water. The mixture of plant extract was heated at 60°C for 10 min. After cooling this solution was filtered through filter paper (Whatman no. 42, Maidstone, England) and stored in refrigerator for further studies [17].

2.3 Synthesis of ZnO nanoparticles

Briefly, 0.1 mM zinc nitrate (ZnNO_3) was prepared with de-ionized water and the volume was made up to 250 ml. After complete dissolution of ZnNO_3 , the flask containing the solution was heated on a water bath at 80°C for 5–10 min. Then, ZnNO_3 solution was mixed with the plant extract under constant stirring. This mixture of the solution was kept at 100°C for 5 h, under vigorous stirring. After this step, a yellow colour precipitate was obtained. This precipitate was discarded through centrifugation (7000 rpm for 15 min). Again, the supernatant was stirred at 150°C for 1 h. Finally the solid pale yellow colour precipitate was derived. The precipitate was purified through washing with de-ionized water followed by methanol and air dried. This product was annealed at 400°C for 2 h. At the end, colourless powder was obtained [17].

2.4 Characterization of ZnO nanoparticles

Optical properties of synthesized ZnO nanoparticles were confirmed by ultraviolet–visible spectroscopy (UV–vis) (UV-2450, Shimadzu) in 200–800 nm wavelength range. The XRD patterns of the synthesized ZnO nanoparticles were carried out using X-ray diffractometer (Perkin-Elmer spectrum one instrument) $\text{Cu-K}\alpha$ radiations ($\lambda = 0.15406$ nm) in 2θ range from 20° to 80°. Fourier transform infrared (FT-IR) spectrometer was used for analysis of functional groups in the synthesized ZnO nanoparticles. FT-IR spectra were recorded in the range 4000–400 cm^{-1} (Perkin-Elmer 1725x), by the KBr pellet method. The synthesized ZnO nanoparticles were analysed for elemental analysis by energy-dispersive X-ray spectrometer (EDX) (RONTEC's EDX system, Model QuanTax 200, Germany). The morphology of the synthesized ZnO nanoparticles were examined by field-emission scanning electron microscope (FESEM) (Model JSM 7610F, JOEL, USA). The powder sample of ZnO nanoparticles average size and size distribution were obtained by high-resolution transmission electron microscopy (HRTEM) (JEOL JEM-3100F).

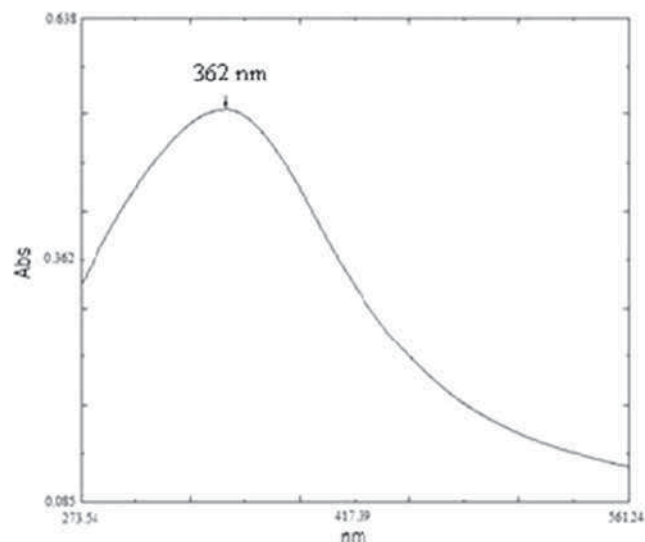


Figure 1. UV spectrum of *L. aculeata*-mediated ZnO nanoparticles.

2.5 Assay for antifungal activity of ZnO nanoparticles

Antifungal activities of the synthesized ZnO nanoparticles were assessed against plant fungal pathogen using a modified Kirby Bauer disc diffusion method [18]. The pathogens were cultured in potato dextrose broth at room temperature on an orbital shaking incubator (Remi, India) at 200 rpm. Aliquot of 100 μl of culture was swabbed on the potato dextrose agar plates using sterile cotton swab. After that plates were allowed to stand for 10 min to allow for culture absorption. The 5 mm size wells were punched into the agar with help of sterile gel puncher. Aliquot of 100 μl (25, 50, 75 and 100 $\mu\text{g ml}^{-1}$) of the ZnO nanoparticles solution and (10 $\mu\text{g ml}^{-1}$) positive control (Amphotericin B) were poured into wells on all plates using micropipette. The plates were incubated in the upside down position at room temperature for 48 h. After incubation period, the zone of inhibition (diameter in millimetre) was measured and the mean values were recorded.

3. Results and discussion

3.1 Synthesis and characterization of ZnO nanoparticles

The UV–visible absorption spectra of the monodispersed ZnO nanoparticles are shown in figure 1. The absorption spectrum of the synthesized ZnO recorded the peak at 362 nm and observed change in colour from brown to pale yellow colour which indicates that the formation of ZnO nanoparticles. Madhumitha *et al* [19] reported that the ZnO nanorods obtained have absorption peak at 364 nm and the band gap of ZnO was found to be 3.32 eV. Qu *et al* [20] stated that the UV absorption spectra for synthesized ZnO was recorded at 370 nm. Similar results were detected by Rajiv *et al* [17].

The functional groups in *L. aculeata* Linn. leaves extract and to identify their role in the synthesis of ZnO

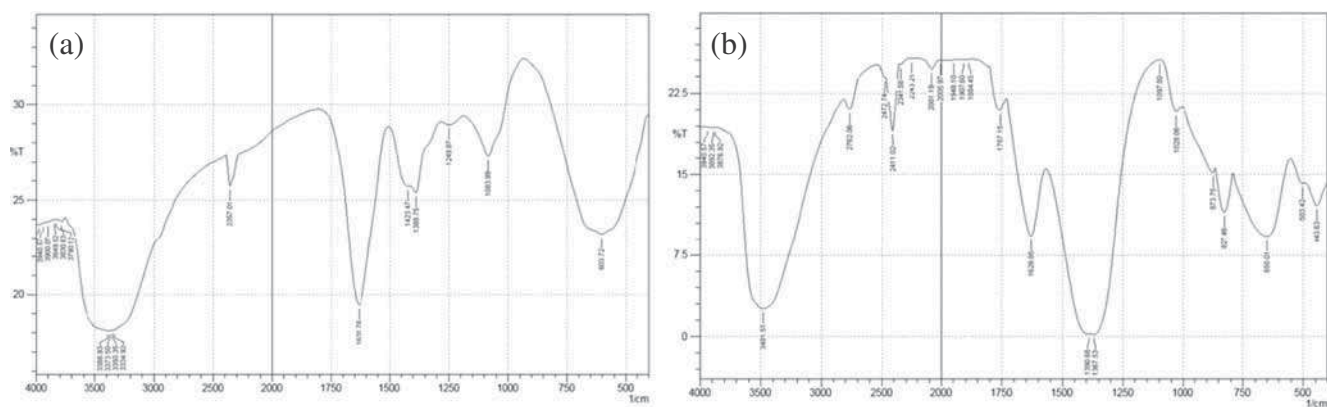


Figure 2. (a) FTIR spectrum of *L. aculeata* leaves extract and (b) FTIR spectrum of *L. aculeata*-mediated ZnO nanoparticles.

nanoparticles by FTIR analysis. The peak in the region from 400 to 600 cm^{-1} is allotted to ZnO [21]. The IR result (figure 2a) of plant extracts shows the spectrum range at 603.72 cm^{-1} which indicates the presence of alkyl halides (C–Br stretch), 1083.99, 1249.87 and 1423 cm^{-1} corresponds to aliphatic amines (C–N stretch) and aromatics (–C–C stretch), 1631.78 cm^{-1} which indicate primary amines (N–H bend), 3334.92, 3350.35, 3373 and 3388.93 cm^{-1} show the presence of alcohols, phenols (O–H stretch). This result shows the presence of phytochemicals such as flavones, quinines and organic acids which are responsible for synthesis of nanoparticles [14].

In figure 2b, IR spectra of synthesized ZnO show a high intensity band around 443.63 cm^{-1} due to the stretching mode of the zinc and oxygen bond [22]. The remaining peak at 1028.06 and 1097.5 cm^{-1} corresponding to aliphatic amines (C–N stretch) 1757.15 cm^{-1} indicates carboxylic acids (C=O stretch) and 3481.51 cm^{-1} represents alcohols, phenols (O–H stretch) in *L. aculeata* extract.

X-ray diffraction was carried out to confirm the phase of ZnO nanoparticles. The peaks at 2θ values of 31.78°, 34.41°, 36.26°, 47.59°, 56.59°, 62.80°, 65.84°, 67.96°, 68.30°, 72.12° and 76.53° corresponded to the crystal planes of (100), (002), (101), (102), (110), (103), (200), (112), (201), (004) and (202) of ZnO nanoparticles. The diffraction peaks could be referred to spherical phase, which were evaluated with the data from JCPDS card no. 89-7102. The strong and narrow peak denotes that the product has well crystalline nature of particles (figure 3). Similar results were reported by Vanathi *et al* [12] in which particles were synthesized using *E. crassipes* leaf extract.

Figure 4 shows the EDX analysis of ZnO nanoparticles 37.22% of zinc and 62.78% of oxygen which confirms the elemental composition of ZnO nanoparticles. The energy-dispersive X-ray analysis (EDX) refers strong signal in the zinc region which confirms the formation of ZnO nanoparticles [23]. The strong signals from the zinc atoms in the nanoparticles recorded and other signals from C and O atoms were observed using EDX analysis in *Parthenium*-mediated ZnO nanoparticles [17]. The EDX analysis display the

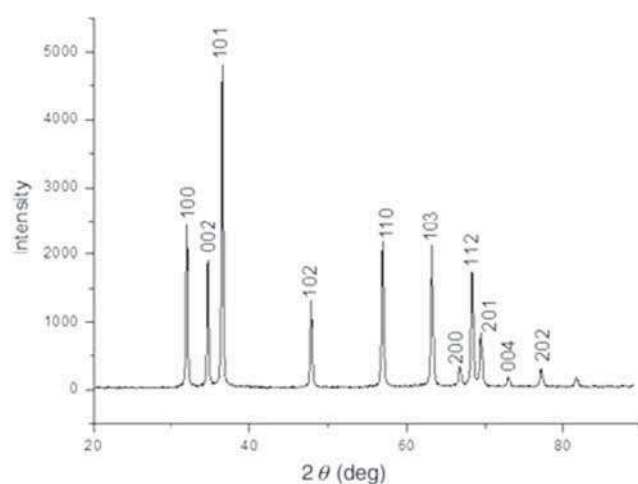


Figure 3. XRD spectrum of *L. aculeata*-mediated ZnO nanoparticles.

optical absorption peaks of ZnO nanoparticles and these absorption peaks were due to the surface plasmon resonance of ZnO nanoparticles [18]. The FESEM images of ZnO nanoparticles are shown in figure 5. From the result it is evident that the morphology of ZnO nanoparticles was spherical in shape and well distributed without aggregation, which is very similar to earlier studies [16]. The size and distribution of the synthesized ZnO nanoparticles were also confirmed by HRTEM (figure 6). It is evident that the particles average size ranged between 12 ± 3 nm and was well dispersed. Similar results were obtained by Vanathi *et al* [12].

3.2 Antifungal activity

The antifungal assay for biologically synthesized ZnO nanoparticles against the pathogens is shown in figure 7. Highest zone of inhibition was obtained in *A. niger* (MTCC: 10180) (21 ± 1.0 mm) and *F. oxysporum* (19 ± 1.0 mm) at a concentration of 100 $\mu\text{g ml}^{-1}$, which is more than positive control (i.e., 12.40 ± 1.00 mm) and which is very similar to

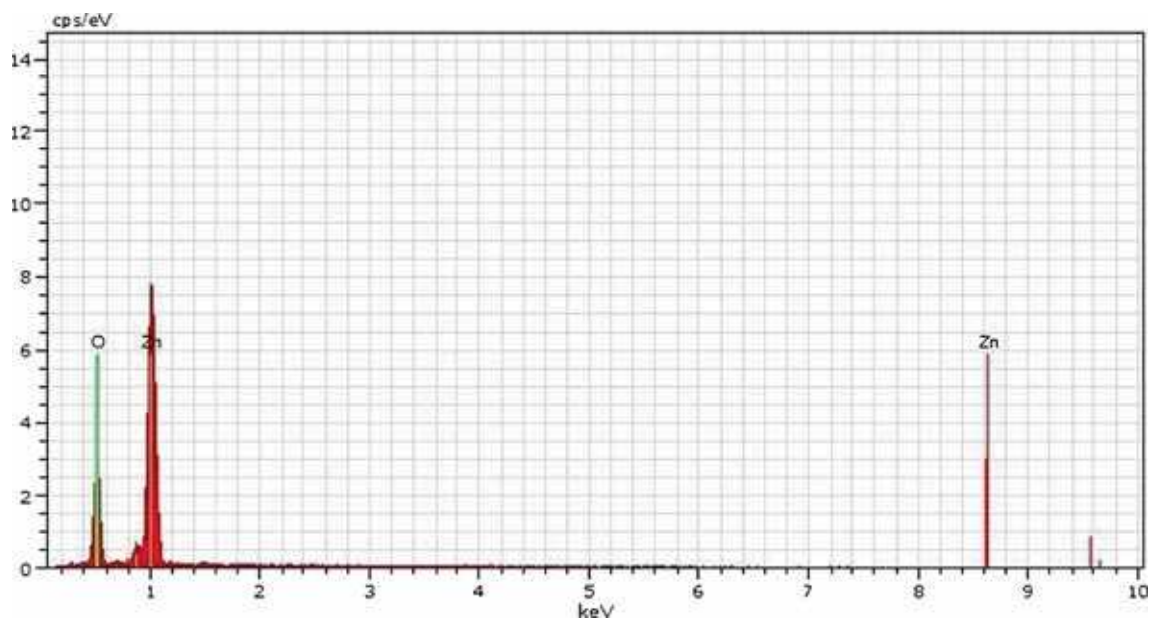


Figure 4. EDX spectrum of *L. aculeata*-mediated ZnO nanoparticles.

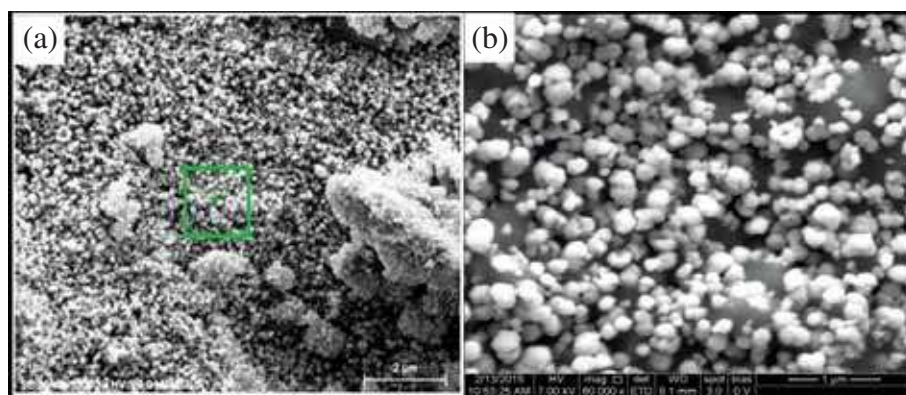


Figure 5. (a and b) FESEM images of *L. aculeata*-mediated ZnO nanoparticles.

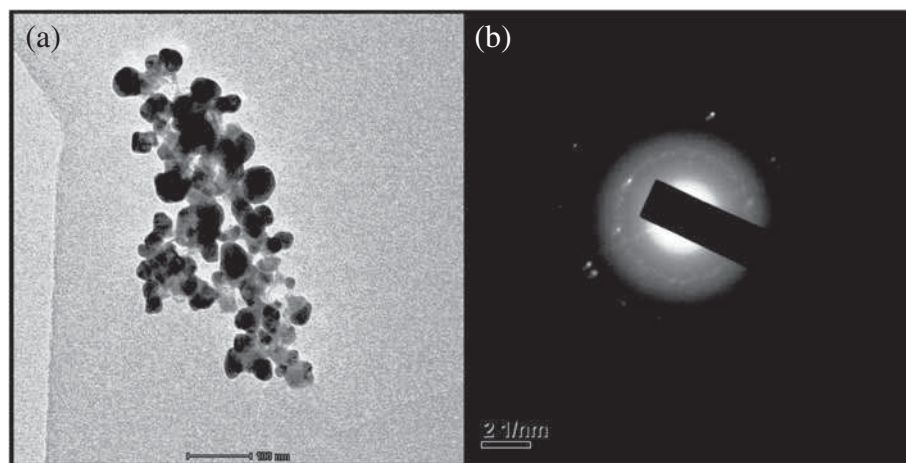


Figure 6. (a) HRTEM images of *L. aculeata*-mediated ZnO nanoparticles and (b) SAED pattern analysis of ZnO nanoparticles.

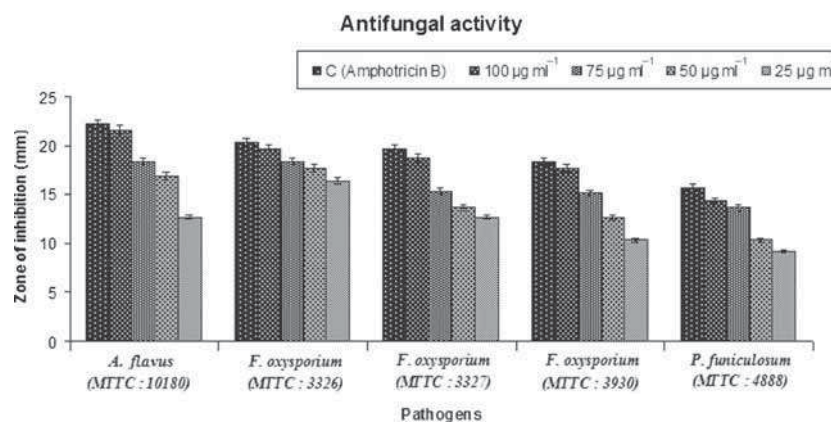


Figure 7. Antifungal activity of *L. aculeata*-mediated ZnO nanoparticles.

previous studies against *A. flavus* (19 ± 1.0 mm) [17]. Lowest zone of inhibition was found in *F. oxysporium* (MTCC: 3930) with a zone diameter of 6.00 ± 1.00 mm at $100 \mu\text{g ml}^{-1}$ concentration of ZnO nanoparticles. The results confirm that biologically synthesized ZnO nanoparticles shows excellent antifungal activity.

4. Conclusion

The present work, green synthesis of ZnO nanoparticles from *L. aculeata* is a green approach, inexpensive, non-toxic and ecofriendly method. All characterization techniques reveal that ZnO nanoparticles were spherical in shape with an average size of 12 ± 3 nm. The synthesized ZnO nanoparticles showed promising antifungal activity against *A. niger*, *F. oxysporium* and *P. funiculosum*. Therefore, these biogenic ZnO nanoparticles could be used as a nanopesticide for improving application of agriculture.

Acknowledgement

We thank the Management of Karpagam Academy of Higher Education, Coimbatore, Tamil Nadu, India, for providing necessary facilities to carry out this work.

References

- [1] Suresh Babu K and Narayanan V 2013 *Chem. Sci. Trans.* **1** 33
- [2] Khorsand Zak A, Razali R, Abd Majid W H and Darroudi M 2011 *Int. J. Nanomed.* **6** 1399
- [3] Ball P 2002 *Nanotechnology* **13** 15
- [4] Nel A, Xia T, Madler L and Li N 2006 *Science* **311** 622
- [5] Roco M C 2003 *J. Nanopart. Res.* **5** 81
- [6] Chen Y B, Koh H J, Park K T, Hiraga K, Zhu Z and Yao T 1998 *J. Appl. Phys.* **34** 3912
- [7] Abhulimen U 2005 *Mater. Res. Soc. Symp. Proc.* **1** 27
- [8] Look D C 2001 *J. Mat. Sci. Eng. B* **80** 383
- [9] Vanaja M, Gnanajobitha G, Paulkumar K, Rajeshkumar S, Malarkodi C and Annadurai G 2013 *J. Nanostruct. Chem.* **3** 17
- [10] Irvani S 2011 *Green. Chem.* **13** 2638
- [11] Mohanpuria P R and Yadav S K 2009 *J. Nanopart. Res.* **10** 507
- [12] Vanathi P, Rajiv P, Narendhran S, Rajeshwari S, Rahman P K S M and Venckatesh R 2014 *Mater. Lett.* **134** 13
- [13] Song J Y J and Kim B S 2009 *Process Biochem.* **44** 1133
- [14] Jha A K P and Prasad K 2009 *Biochem. Eng.* **43** 303
- [15] Ghisalberti E L 2000 *Fitoterapia* **71** 467
- [16] Rajendiran K, Soumiya D and Sudaroli Sudha J 2014 *Int. J. Food Agric. Vet. Sci.* **4** 165
- [17] Rajiv P, Rajeshwari S and Venckatesh R 2013 *Spectrochim. Acta Part A* **112** 384
- [18] Ankanna S and Savithamma N 2011 *Asian J. Pharm. Clin. Res.* **4** 137
- [19] Madhumitha R, Karthikka P and Navin Kumar S 2014 *J. Global Biosci.* **3** 415
- [20] Qu J, Luo C and Hou J 2011 *Micro. Nano. Lett.* **6** 174
- [21] Tas A C, Majewski P J and Aldinger F 2002 *J. Am. Ceram. Soc.* **85** 1421
- [22] Kwon Y J, Kim K H, Lim C S and Shim K B 2002 *J. Ceram. Proc. Res.* **3** 146
- [23] Vanheusden K, Seager C H, Warren W L, Tallant D R and Voigt J A 1996 *Appl. Phys. Lett.* **68** 403